ChemPubSoc Europe

DOI: 10.1002/cphc.201500231

CHEMPHYSCHEM Concepts

Thermodynamics and Kinetics of Prenucleation Clusters, Classical and Non-Classical Nucleation

Dirk Zahn*[a]

Recent observations of prenucleation species and multi-stage crystal nucleation processes challenge the long-established view on the thermodynamics of crystal formation. Here, we review and generalize extensions to classical nucleation theory. Going beyond the conventional implementation as has been used for more than a century now, nucleation inhibitors, precursor clusters and non-classical nucleation processes are rationalized as well by analogous concepts based on competing interface and bulk energy terms. This is illustrated by recent examples of species formed prior to/instead of crystal nucleation and multi-step nucleation processes. Much of the discussed insights were obtained from molecular simulation using advanced sampling techniques, briefly summarized herein for both nucleation-controlled and diffusion-controlled aggregate formation.

1. Introduction

Since the seminal work of Ostwald in the late 19th century, crystal nucleation and growth have remained of constant, if not even increasing, interest.[1] Today, applications of crystal engineering range from quantum dots and nanomaterials to biomimetic composites and pharmaceutical formulation. In parallel to pushing the limits of creating new materials by brute-force methods such as high-throughput screening robots, we are experiencing considerable improvements in experimental investigation techniques[2] and simulation methods.[3] The combination of both types of characterization approaches is currently paving the way to an increasingly rational design of crystalline compounds. The key to this highly desirable, but still rather far-off goal is an in-depth understanding of the processes involved at a molecular scale.

The need for molecular-scale understanding has increased sharply recently, as the observation of multi-stage nucleation processes and the identification of prenucleation clusters challenges our current theoretical mainframe for rationalizing the underlying thermodynamics. For such phenomena, the traditional concept of classical nucleation theory faces serious shortcomings[4,5]—and ultimately motivated the term "non-classical nucleation". To exploit new perspectives of solid-state syntheses by designing precursor solutions and/or triggering secondary nucleation events, extensions to classical nucleation theory are required.

[a] *Prof. Dr. D. Zahn*
Lehrstuhl für Theoretische Chemie/Computer Chemie Centrum
Friedrich-Alexander Universität Erlangen-Nürnberg
Nägelsbachstraße 25, 91052 Erlangen (Germany)
E-mail: dirk.zahn@chemie.uni-erlangen.de

The aim of the present concept article is to provide a survey on the thermodynamics of nucleation, be it multi-step or straight (e.g. "classical"), also considering the recently identified prenucleation clusters. Moreover, we briefly discuss kinetics, experimental and numerical simulation methods that have proven to be valuable tools for rationalizing the molecular-scale processes involved in solute association, cluster/nuclei formation and the growth of crystals.

2. Classical and Non-Classical Nucleation

A simple and intuitive rationalization of crystal formation was provided by Gibbs, who contrasted two key driving forces, one of which promotes and one that disfavors the formation of a crystal.[6,7] From a purely thermodynamic point of view, crystallization should occur when super-saturation, under-cooling or pressure causes the crystalline phase to be more stable than the corresponding solution or melt, respectively. However, immediate phase transfer is typically observed only upon rather drastic favoring of the crystalline state, as for example by vaporization of the solvent. Unlike crystal formation by a manifold of spontaneous nucleation events (spinodal decomposition of the pristine phase), the more common scenario is that of crystal formation being hindered by a barrier in free energy. Classical nucleation theory (CNT) relates this barrier to the need of a forming crystal nucleus to establish an interface with the surrounding melt, vapor or solution. Surface tension and unfavorable interactions at the interface give rise to an increase in free energy, which scales with the surface area A of the forming nucleus. On the other hand, favorable interactions within the inner core of the forming nucleus lead to a prospective gain in free energy, which scales with the volume V of the nucleus. The central merit of CNT is to describe the competition of both aspects by two simple terms in order to provide an energy profile as a function of nucleus size. In what follows,

$G(N)$ is considered as the free energy difference in comparing the dispersed solution comprising N solutes with an analogous system in which all N solutes form an aggregate and are embedded by equal amounts of solvent molecules and modeled at identical temperature and pressure as considered for the dispersed solution [Eq. (1)]:

$$G(N) = g_{\text{surface}}(A) - g_{\text{bulk}}(V) \quad (1)$$

For spherical nuclei the two energy terms may be written as a function of the radius, but a shape-independent formulation of CNT may be obtained by considering the surface and the bulk energy terms as a function of the number of solutes N in the nucleus. Assuming the inner structure of the nucleus as identical to that of the final crystal, the gain in free energy upon crystallization reads $-\mu{\cdot}N$ with μ being the change in free energy per solute. A further assumption often used relies on the nuclei to maintain a constant shape (such as spheres, cubes, prisms, polyhedra, etc.) during the whole formation process. In this case the surface area is given by $f{\cdot}N^{2/3}$ with f being a constant that depends on the habit of the nucleus. For example, a spherical shape would lead to Equation (2):

$$N = \rho \cdot \frac{4}{3}\pi r^3 \quad \text{and} \quad A_{\text{surface}} = 4\pi r^2 = \left(\sqrt[3]{36\pi} \cdot \rho^{-2/3}\right) \cdot N^{2/3} \quad (2)$$

where ρ refers to the particle density of the forming crystal. This allows describing nucleation free energy as a function of the number of precipitated solutes [Eq. (3)]:

$$G(N) = c_{\text{surface}} \cdot N^{2/3} - \mu \cdot N \quad (3)$$

from which the nucleation barrier and the critical nucleus size is deduced as Equation (4):

$$0 = \left.\frac{\partial G(N)}{\partial N}\right|_{N_{\text{crit}}} \rightarrow N_{\text{crit}} = \left(\frac{2c_{\text{surf}}}{3\mu}\right)^3; \quad \Delta G = \frac{4}{27}\frac{c_{\text{surf}}^3}{\mu^2} \quad (4)$$

It is important to point out that both the surface and the volume terms are related to constant prefactors c_{surface} and μ, respectively. On this basis, CNT provides a simple rationale of the free energy profile as a function of size (Figure 1 a). Results should, however, be regarded from a more qualitative viewpoint as there are a number of examples that show the shortcomings of assuming constant shape and inner structure of the nuclei as discussed in the following.

Molecular simulation studies have proven particularly valuable for extending our mechanistic understanding beyond classical nucleation theory. On the one hand, this applies to the surfaces of forming nuclei: to minimize interfacial free energy, diffusive and dynamically changing nucleus–melt or nucleus–solvent interfaces appear more favorable.[8] However, an even more important issue is the need to consider structural transitions within the inner core of a forming crystal. First evidence for this was collected by Ostwald, leading to the famous Ostwald's step rule which suggests a series of structural transitions during crystal nucleation.[1] While the original argument was based on preferential nucleation of a phase that is structurally similar to the preceding one, a more thermodynamic rationale of multi-step nucleation processes is given by following the pathway encompassing the lowest nucleation barrier.[1,9] The latter criterion can be considered as a qualification of the former, if "structural similarity" of two phases is interpreted in terms of the ease to transform the one into the other.

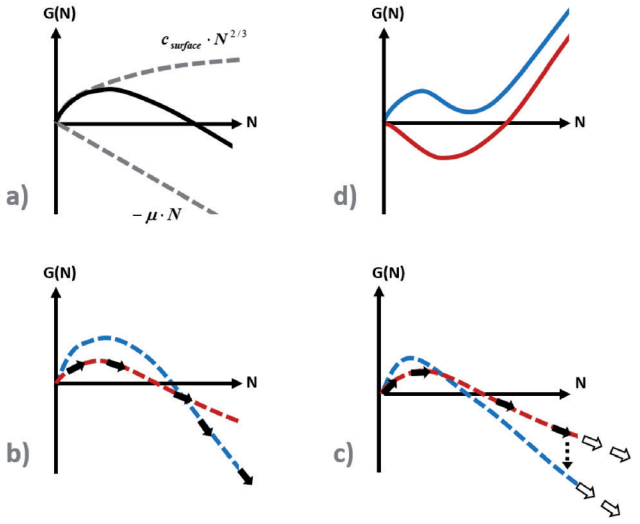

Figure 1. a) Classical nucleation pathway: small nuclei are dominated by interface/surface domains accounting for an increase in free energy, whilst sufficiently large nuclei are stabilized from favorable packing in the bulk, leading to a net gain in free energy. b) Two-step nucleation mechanism with low secondary nucleation barrier: the initially formed phase A (red curve) is that of lowest nucleation barrier, that is, nuclei of comparably low surface tension/interface energy are observed. Upon later stages of nuclei growth the core domain in the aggregate becomes dominant and transformation to phase B (blue curve) is driven by more favorable packing in the bulk. c) Competition of crystal structures with large barriers to polymorphic transitions: same as (b) but for weaker thermodynamic preference of the A→B transition and/or larger barrier to the secondary nucleation event. The size-induced transformation may be subject to large hysteresis effects or even inhibit structural reorganization at all. d) Prenucleation clusters: non-constant bulk and surface/interface energy terms may lead to (local) minima in the energy profile and give rise to *meta*-stable (blue curve) or even stable (red curve) prenucleation clusters.

3. Multi-Step Nucleation and Crystal Polymorphism

An important example of two-step nucleation is given by solute segregation in terms of a single disordered cluster or a partially ordered agglomerate of clusters, followed by aggregate ordering at a later stage of the precipitation process.[10–13] An explanation of such non-classical nucleation may indeed be given by considering the competition of (at least) two phases.[4] Here, the final crystal structure implies most favorable solute packing in the bulk and is thus the predominant phase for large crystal nuclei. On the other hand, the formation of disordered clusters could give rise to roughly spherical aggregates of particularly favorable surface tension and/or interface energy. In this case, the disordered structure is thermodynamically preferred for small aggregates, whilst the crystalline

structure is only stable for larger aggregates. Illustrations for such two-step nucleation are given in Figures 1 b,c.

It is noteworthy that the secondary nucleation step requires a size-induced phase transition of the forming aggregate. Depending on the solute, such liquid–solid or solid–solid transformations may be subject to a considerable energy barrier. As a consequence, hysteresis effects might shift the secondary nucleation step to late stages of aggregate growth or even fully inhibit transformation to the thermodynamically preferred structure. A prominent example of the latter case is given by molecular crystals, which are particularly often found to nucleate in terms of different polymorphic structures depending on the specific synthesis conditions (and thus different rankings of the corresponding nucleation barriers).

By means of molecular simulation we can monitor the evolution of a forming molecular crystal nucleus as a function of size. This is particularly insightful for multi-step nucleation mechanisms. An example is given in Figure 2, which shows

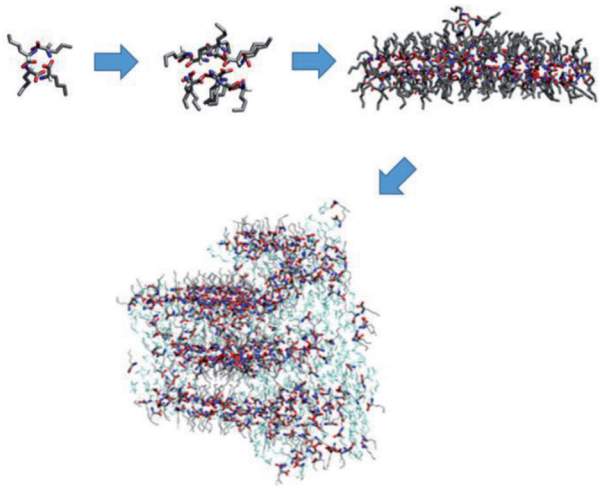

Figure 2. Evolution of a forming molecular crystal of D-/L-norleucine as obtained from molecular simulation.[14] In nonpolar (octanole) solvent, the solutes initially form hydrogen-bonded micelles and bilayers. At later stages, additional bilayers nucleate from the pristine structure and aggregates of staggered bilayers are observed. This multi-step nucleation mechanism hence encompasses a series of solid–solid transformations between competing structures of size-dependent thermodynamic stability.

a series of snapshots of norleucine aggregation from a nonpolar solution.[14] The initial oligomers are associated by hydrogen bonding, whilst the nonpolar alkyl chains point towards the aggregate surface. This micelle-type structure evolves to hydrogen-bonded bilayers upon incorporation of up to about 150 molecules. At later stages, the transition from two-dimensional to three-dimensional aggregates is observed, eventually leading to staggered bilayers akin to the final crystal structure. However, even upon aggregate growth to 1000 solutes, the evolution of the investigated D-/L-norleucine aggregates is still incomplete as the transformation of hydrogen-bonded dimer motifs to enantiopure chains still gives rise to solid–solid transformations.[14] This example hence shows that during the nucleation of D-/L-norleucine a cascade of structural transitions (micelles→bilayers→staggered bilayers→molecular crystal) is experienced. Each of the competing structures refer to different surface tension and bulk energy terms, leading to size-dependent thermodynamic stability, which is suggested as the driving force for the observed multi-step nucleation pathway.

4. Prenucleation Clusters and Nucleation from Building Blocks

Similar to the size-dependent phase stability discussed earlier for nuclei of competing crystal polymorphs, the structures and energetics of non-crystalline clusters need to be considered as functions of size as well. This gives rise to a variety of challenges to conventional CNT and the required extensions of the theory mainframe are still under development. Schematically, prenucleation clusters may occur in terms of 1) relatively favorable, yet thermodynamically unstable, intermediates to crystal nucleation (Figure 1 d). Long-standing examples for discontinuous size dependence in cluster energy are magic-number clusters observed during metal crystallization from the vapor.[15,16] Molecular dynamics simulations showed that the evolution of forming metal nuclei involves structural transitions from nuclei with crystalline bulk to compact polyhedra of particularly favorable surface tension and vice versa.[16]

On the other hand, 2) prenucleation clusters may also occur as the thermodynamically favored species with respect to the dispersed solutes. The term "stable" is then used to describe prenucleation clusters that coexist with dispersed solutes in solutions below the saturation limit. A simple example of such a solution is given by tenside molecules in water. Here, the formation of micelles may be rationalized by a favorable interface energy term and unfavorable bulk energy, thus flipping the chart characteristic to conventional CNT (compare Figures 1 a and d). Comparing micelles with dispersed tenside molecules, favorable interface energy arises from the segregation of hydrophobic moieties. On the other hand, unfavorable bulk (free) energy results from insufficient solute–solute interactions compared to the entropy change needed for solute aggregation. A similar argument might apply to the most popular type of prenucleation clusters, that is, clusters that are coordinated by surfactants—a prominent example being $Zn_4O(acetate)_6$ clusters observed in ethanolic solutions of zinc acetate dihydrate.[17–19] In such systems, the coordination by surfactants obviously lowers the interfacial energy of the clusters. We are however not aware of a rigorous proof of thermodynamic stability (which would refer to case 2) and kinetic hindering could also account for preventing ripening to ZnO.

While the (relative) stability of the cluster types discussed above is intuitive and has been well-established for many decades, the recent discovery of an unexpected type of prenucleation species considerably extended our picture of solutions prior to nucleation. Using ultracentrifugation, Coelfen and Gebauer identified $CaCO_3$ prenucleation clusters in aqueous solution.[20] In absence of surfactants, the rationale based on micelles does not apply. On the other hand, arguments based on specific structures of preferential energy such as the magic-number clusters observed for metals also appear unreasonable as $CaCO_3$ is known to (initially) nucleate as amorphous aggregates. On the basis of molecular simulations Wallace and

De Yoreo instead suggest the formation of liquid-like droplets of high ion concentration.[21] Therein, polyionic chains account for favorable interactions in the bulk, whilst the interfacial energy between the ion-rich and the ion-poor solutions appears as practically zero.[22,23]

An initially prepared dispersed solution of calcium carbonate below the saturation limit would therefore undergo spinodal decomposition to form the suggested liquid-like prenucleation species.[24] Interestingly, experiments do not show separation into two entirely distinct phases, indicating that the liquid-like droplets of high ion content are limited in size. Assuming vanishingly low, but clearly not negative interface tension, limitations to the droplet size can only be a consequence of a size-dependent term for the free energy of the aggregate bulk. On the one hand, this might be due to the loss in entropy arising from changing a micro-elusion-type scenario into that of a large single droplet. Additionally, a possible rationale could build on the study of Gale and coworkers who found that amorphous $CaCO_3$ incorporates an increasing number of water molecules per $CaCO_3$ formula unit with increasing aggregate size.[22] This implies an increasing degree of immobilized water molecules, giving rise to entropic disfavoring. We suggest that a similar mechanism might account for limiting the size of the liquid-like poly-ionic chains. Short ion chains are essentially linear and bind only water molecules of the first hydration shell, whilst larger droplets imply extended networks of nested poly-ionic chains that would encapsulate water and are thus subject to increasingly unfavorable entropy. Unfortunately, molecular dynamics simulations could so far only hint at the first part of this concept,[23] whereas the latter part is still speculation, inspired by the swelling of ionic polymer compounds.

It is tempting to interpret crystal nucleation via prenucleation clusters as a special case of the non-classical nucleation pathways discussed earlier. In this sense, the first nucleation step would be the agglomeration of prenucleation clusters, forming (partially) organized structures which could also be interpreted as *meso*-crystals.[25] The secondary nucleation step then refers to the ripening of such agglomerates into the final crystal structure.[24] An exciting perspective of such nucleation pathways is to manipulate crystal nucleation by selection of the prenucleation species acting as building blocks. This would allow promoting specific structural motifs and ideally directing crystal nucleation into specific polymorphs or compositions.

Using cyro-TEM Sommerdijk and Faivre recently provided strong evidence for this concept by capturing different stages of iron oxide/hydroxide agglomeration from solution, followed by a secondary nucleation event leading to magnetite crystals.[26] As thermodynamic rationale, these authors suggested to use classical nucleation theory as developed for nucleation from disperse solution (Figure 1 a), but to introduce an offset in terms of size and free energy to describe nucleation from precursor clusters. This offset directly corresponds to the (local) minima in the free energy profiles illustrated in Figure 1 d.

The key question is whether such offsets to the free energy level of the solution indeed lead to lower effective nucleation barriers (as evidently the case for the above study on magnetite). Nucleation from particularly favorable solute clusters could instead imply an increase in the free energy barrier as compared to the dispersed solution. In this case, the putative precursor clusters actually reflect nucleation inhibitors. We argue that this depends on the *crossing of the free energy profiles* related to the prenucleation clusters with the energy curve corresponding to conventional nucleation from solution. Figure 3 illustrates the three possible scenarios depending on the degree of thermodynamical stability and the size distribution of the prenucleation clusters compared to the critical nucleus estimated from classical nucleation theory. Metastable prenucleation clusters may be interpreted as relatively favorable intermediates to crystal nucleation and are thus well-suited as building blocks to non-classical crystal nucleation. For clusters that are thermodynamically preferred over solutions of dispersed solutes the picture is more complex.

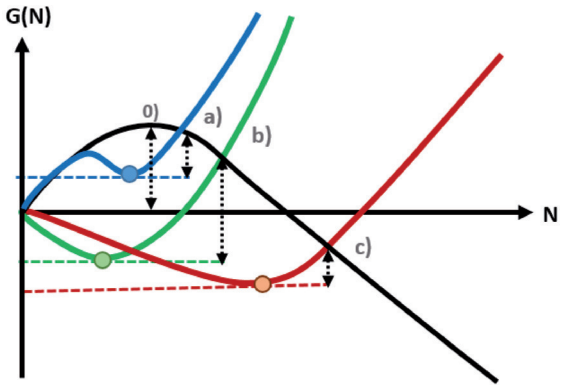

Figure 3. Crystal nucleation from prenucleation clusters: the black curve refers to classical nucleation of a crystal from a solution of dispersed ions and the colored curves illustrate the possible energy profiles for prenucleation clusters. The blue curve corresponds to a metastable prenucleation cluster which may be interpreted as a relatively favorable intermediate to crystal nucleation. The effective barrier to crystal formation (a) is lower than that of conventional nucleation from the ionic solution (0). For stable prenucleation clusters, two scenarios may apply: large prenucleation clusters of broad size distribution can imply low effective barriers to crystal nucleation (c) and may thus serve as precursors to crystal formation. On the other hand, small prenucleation clusters of sharp size distribution would imply an increase in effective nucleation barrier (b). In this case, crystal nucleation appears more favorable in regions of the ionic solution, initially not affecting the prenucleation clusters.

The free energy diagrams shown in Figure 3 illustrate two different types of such clusters. Here, only the example of large prenucleation clusters of broad size distribution exhibits a low effective barrier to crystal nucleation, thus qualifying the clusters as building blocks to crystal formation. (Note that the crossing of the free energy curves only reflects a rough estimate of the transition barrier and that it ignores the possibly quite large increase in energy barrier arising from cluster reorganization.) Contrary to this, the illustrated curve for small prenucleation clusters of sharp size distribution indicates a considerable barrier for the cluster→nucleus transition (even using the lower estimates as obtained from Figure 3). For the given example, this barrier is even larger than the barrier to nucleation from bulk solution. Consequently, nucleation is expected to take place within the bulk ionic solution without affecting the previously formed clusters and the term "prenucleation

cluster" is misleading. Indeed, this type of cluster formed prior to nucleation would persist until later stages of crystal growth as described next.

Clusters that are the most stable species present in solution prior to crystal nucleation may still be outperformed thermodynamically once the nuclei reach mature stages of crystal growth. The critical point is the intersection of the free energy gain from solute uptake in post-critical crystal nuclei compared to the free energy of the same number of solutes within the previously formed clusters (Figure 4, green curve). The fate of

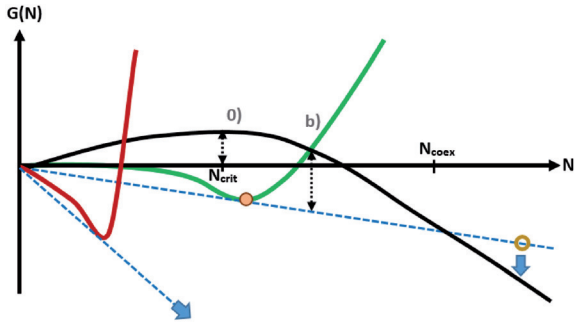

Figure 4. Free energy diagram for crystal nucleation from solution of dispersed solutes (black curve, barrier denoted as 0) initially ignoring the clusters formed prior to nucleation (green curve, barrier to direct transformation denoted as b). Such clusters would coexist with (post-critical) crystal nuclei of small size ($N_{crit} < N < N_{coex}$). However, at more mature stages of crystal growth, the free energy gain in solute association to the growing nucleus may outperform thermodynamic preference of solute assembly in a single or multiple (here shown for 2) clusters. On the other hand (red curve), excessive stabilization of small clusters in solution may actually inhibit crystal nucleation. The dashed blue lines indicate the free energy of multiples of clusters taken as a simple linear extrapolation of the cluster of most favorable size.

the beforehand stable clusters in solution then is to either 1) collide with a forming nucleus and merge into it; or alternatively 2) the clusters might dissociate into solution to compensate for the depletion of dispersed ions in the solution arising from crystal precipitation. The choice of mechanisms also depends on cluster mobility compared to the diffusion of dispersed ions. Interestingly, the mechanistic picture 2 is similar to the Ostwald ripening[27] of differently sized crystal nuclei. Particularly for this scenario we argue that the clusters formed prior to nucleation should be regarded as buffers to ion concentrations in solution rather than precursors to crystal nucleation. On the other hand, route 1 implies that the clusters are candidate building blocks to crystal growth, but not to nucleation.

From a practical point of view, crystal design from precursor solutions is probably most promising for two-step processes. In the first step, particularly stable, well-defined clusters are formed prior to nucleation. By changing the solution (e.g. adding a further component etc.) the cluster stability is then reduced to provide a more reactive species that agglomerate and turn into crystal nuclei. The above-mentioned $Zn_4O(acetate)_6$ clusters in ethanolic solution are prominent examples for this strategy. In the initial solution, these clusters are quite stable and the nucleation of ZnO is typically triggered by adding hydroxide.[17] In analogy to this, Mehring and coworkers prepared DMSO solutions of $[Bi_6O_4(OH)_4](NO_3)_6$ cage structures as precursors to larger bismuth oxide aggregates.[28] Using molecular dynamics simulations we identified the mechanisms of precursor stabilization by coordinating nitrate ions.[29] For intact $[Bi_6O_4(OH)_4](NO_3)_6$ clusters the nitrate surfactants were shown to electrostatically inhibit the association of the clusters, thus giving rise to stable solutions. However, by lowering the pH, the clusters may be protonated and dissociation of a HNO_3 molecule leads to the formation of an activated species, the $[Bi_6O_4(OH)_4](NO_3)_5^+$ cluster, which was found to bind several $[Bi_6O_4(OH)_4](NO_3)_6$ clusters. The first association event and the resulting dimer after structural ripening are illustrated in Figure 5. Interestingly, the newly formed $[Bi_{12}O_8(OH)_8](NO_3)_{11}^+$ cluster still refers to an activated species and was shown to bind further precursor clusters in order to grow into a crystal nucleus. We argue that the pristine $[Bi_6O_4(OH)_4](NO_3)_6$ refer to clusters that were thermodynamically preferred species in the initial solution, whilst the activated species evidently correspond to metastable intermediates to crystal nucleation.

An extreme case of promoting the stability of small clusters in solution is reflected by the free energy profile shown as the red curve in Figure 4. In this case, the cluster species is thermodynamically preferred over the bulk crystal and the solution would rather form multiples of clusters than a crystal. An illustrative example for this scenario is polyacrylate additives in aqueous solution used to hinder $CaCO_3$ nucleation. Combing molecular dynamics simulations with an extensive structural sampling technique, Parinello and coworkers demonstrated the peculiar binding of calcium and carbonate ions to the additive.[30,31] Despite the local accumulation of ions, crystal nucleation is still disfavored as the association with the polyacrylate additive leads to Ca–Ca distances that mismatch with the packing in any of the known solid forms of calcium carbonate.

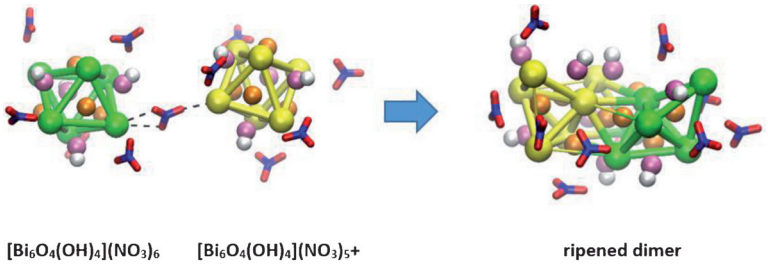

Figure 5. Association of $[Bi_6O_4(OH)_4](NO_3)_6$ (left) to an activated $[Bi_6O_4(OH)_4](NO_3)_5^+$ precursor cluster. The initially formed salt-bridges between nitrate and exposed Bi ions were found to ripen in favor of $[Bi_{12}O_8(OH)_8](NO_3)_{11}^+$ cluster (right). The ripened dimer shows a central Bi_6 octahedron with which Bi_4 tetrahedra are associated, giving rise to favorable (bulk-like) four-fold coordination of the O^{2-} ions, whilst the OH^- ions are located at the aggregate boundaries only. Pictures were taken from molecular dynamics simulations as reported in Ref. [29]. Reproduced with permission from Wiley-VCH.

5. Conclusions

There is no way to opt out of thermodynamics. Crystal nucleation processes called non-classical elude the concept of classical nucleation theory in its conventional implementation, but classical mechanics and statistics nevertheless apply. Indeed, the almost 150 year old concept of classical nucleation theory only requires small extensions to account for the manifold of nucleation and prenucleation phenomena known today.

Multi-step nucleation processes may be rationalized by considering multiple free energy profiles, each derived in a classical manner, that is, by contrasting unfavorable surface/interface tension to favorable bulk energy. The nucleation process will follow the route with lower barriers, which may arise from low interface tension rather than optimal bulk energy. In this case, size-induced changes in polymorph stability may be predicted from the crossing of the free energy profiles of competing crystal structures. The actual solid–solid transition is subject to a kinetic barrier, which implies hysteresis or even prevents the direct transformation at all.

We argue that clusters formed prior to nucleation should be divided into two categories. The presence of metastable clusters can lower the barrier to nucleation as compared to the dispersed solution. This cluster species thus represent possible precursors to crystal nucleation. On the other hand, the term prenucleation cluster seems inappropriate for clusters that are thermodynamically more stable than the dispersed solution. Crystal nucleation from such clusters might involve even larger barriers, giving rise to a hindering rather than a boosting effect.

Theory and Computational Methods

Nucleation Kinetics versus Diffusion-Controlled Crystal Formation

For classical crystal nucleation pathways corresponding to the energy profile illustrated in Figure 1a the kinetics may be estimated from the rate of critical nucleus formation. Rate theory[32] implies [Eq. (5)]:

$$r_{\text{nucleation}} = r_0 \cdot \exp\left(-\frac{\Delta G}{k_B T}\right) \tag{5}$$

where T is temperature, k_B the Boltzmann constant and r_0 denotes the kinetic prefactor, respectively. Processes that determine the kinetic prefactor are solute diffusion in solution and solute desolvation in order to incorporate the solute in the forming nucleus. Both of these processes are typically related to an activation energy stemming from the need to rearrange solvation shells or replacing solvent–solute by solute–solute contacts. Formally, the kinetic prefactor may thus be written as Equation (6):

$$\begin{aligned} r_0 &= r_{\text{diff}} \cdot r_{\text{desolv}} \\ r_{\text{diff}} &= r^0_{\text{diff}} \cdot \exp\left(-\frac{\Delta E^{\text{diff}}}{k_B T}\right) \\ r_{\text{desolv}} &= r^0_{\text{desolv}} \cdot \exp\left(-\frac{\Delta E^{\text{desolv}}}{k_B T}\right) \end{aligned} \tag{6}$$

When combining Equations (5) and (6) it is tempting to combine the three exponential terms into a putative effective barrier $\Delta G + \Delta E^{\text{diff}} + \Delta E^{\text{desolv}}$, which is, however, quite misleading as diffusion, desolvation and nucleation are separate steps. This is best seen from considering the rate of critical nucleus dissociation during a failed attempt to nucleation [Eq. (7)]:

$$\begin{aligned} r_{\text{crit}\rightarrow\text{desolv}} &= r_0 \cdot \exp\left(+\frac{\Delta G}{k_B T}\right) \\ &= r^0_{\text{desolv}} \cdot r^0_{\text{diff}} \cdot \exp\left(-\frac{\Delta E^{\text{diff}}}{k_B T}\right) \exp\left(-\frac{\Delta E^{\text{desolv}}}{k_B T}\right) \exp\left(+\frac{\Delta G}{k_B T}\right) \end{aligned} \tag{7}$$

Indeed, solute diffusion and de-/resolvation processes always impose a barrier that slows the kinetics, be it the forward or the backwards reaction. This motivated the interpretation of ΔE^{diff} and ΔE^{desolv} as kinetic barriers, whilst ΔG is called the thermodynamic barrier.[33]

In view of the different process steps and their corresponding activation barriers, it is useful to discriminate the two limiting cases of diffusion-controlled and nucleation-controlled crystal formation. The latter type of processes is characterized by $\Delta G \gg \Delta E^{\text{diff}} + \Delta E^{\text{desolv}}$. On the other hand, diffusion-controlled crystal formation implies no or only low barriers to desolvation and nucleation, but not necessarily $\Delta E^{\text{diff}} \gg \Delta G + \Delta E^{\text{desolv}}$. Indeed, diffusion will always become rate-determining if solubility is low and nucleation occurs from very sparse solution. The two limiting scenarios—crystal growth limited by mass transport to the nucleus and nucleation triggered by crossing an activation barrier—give rise to rather different challenges to both experiment and molecular simulation.

A broad overview of experimental techniques for characterizing nucleation processes was recently provided by Bensch et al. and the reader is directed to Ref. [2] for a detailed account. Moreover, a topical survey of experimental approaches to clusters formed prior to nucleation and non-classical nucleation was provided by Gebauer and Coelfen.[5] In the following, we give a brief summary of molecular simulation methods which, in combination with experimental characterization, reflect the state-of-the-art in unraveling clusters, precursors and nuclei in solution.

Molecular Dynamics Simulation Approaches to Understanding Crystal Nucleation

Molecular dynamics simulations reflect iterative solutions to Newton's equations of motion and thus calculate molecular trajectories as small increments of time. While this time step (and hence the maximum time resolution) is typically around 1 fs, the overall simulation time is usually chosen within the ns to μs regime. These time scales require millions of simulation iterations, but are still substantially lower than that of most nucleation process of experimental or industrial relevance. Using specialized simulation techniques for bridging the time/length scale problem, crystal nucleation may still be assessed by molecular simulation as briefly summarized in the following (for a more detailed account see Ref. [3]). While the techniques discussed apply to all types of molecular dynamics simulations, we note that the atomic interaction forces are most accurately calculated from quantum treatment of the electrons, and specifically developed molecular mechanics models are needed to obtain similar accuracy. The latter are usually preferred, as force fields allow for assessing larger systems and longer time scales and thus provide drastically lower margins of the statistical error.

For nucleation-controlled processes, the key barrier arises from ordering a domain within the melt or from desolvation and rearranging nearby solutes within a solution. To make such processes accessible to molecular simulation, the strategies developed, in one way or another, are all based on first implementing an artificial boost of solute–solute interactions, and then correcting the biasing of the results. Frenkel and coworkers pioneered this field by driving nucleation from the melt via a predefined order parameter that reflects nearest-neighbor distances and angles.[34–36] To avoid bias from excessively boosting nucleation kinetics, the process is described by a series of setups each mimicking the steady state within a small interval of the order parameter. Using the umbrella sampling technique, artificial potentials were implemented to restrain the order parameter within a certain range, and sketches of the energy profile (potential of mean force) were collected from Boltzmann statistics.[34–36]

While umbrella sampling uses additional potentials to create attraction towards a desired state to the model system, it is also possible to induce nucleation processes by artificially creating repulsion from an unwanted configuration. The metadynamics technique reflects a systematic scan of configuration space by continuously disfavoring configurations that have been characterized before. This approach does not require prejudicing a reaction coordinate (as in umbrella sampling), but relies on a broader a set of predefined variables to which the biasing potential is applied. Within this choice of descriptors, metadynamics samples configuration space free of prejudicing.[37]

More recently, transition-path-sampling molecular dynamics was employed to sample time-dependent pathways of nucleation from solution.[38,39] Here, an initial nucleation pathway is prepared from imposing high temperature, pressure or manipulation of the interaction potentials.[40] Increasingly realistic pathways are then collected from performing a Monte Carlo sampling within trajectory space confined to liquid–solid transition routes. By the example of NaCl aggregation in water, this approach was also tested for investigating nucleation from solution.[41]

To study diffusion-controlled crystal formation processes, an alternative class of simulation methods proved more performing. The general concept is to treat solute diffusion and solute aggregation by different methods. Gavezzoti pioneered this field by essentially ignoring long-range diffusion process and exploring the manifold of solute–solute contacts from small model systems comprised of only a few solutes.[42,43] This allows focusing molecular simulation to the critical issue of solute–solvent bond dissociation and replacement by solute–solute bonds. Possible crystal structures are then predicted from expanding the manifold of solute–solute contacts to periodic arrangements.[43]

The Kawska–Zahn method describes solute diffusion to a forming nucleus by an inexpensive docking procedure implemented as a Monte Carlo step, whilst solute association and the reorganization of the aggregate is studied from explicit molecular dynamics simulations.[44] Depending on the model system, aggregate relaxation after each growth step can be modeled in different ways. 1) From direct molecular dynamics simulation of a given period of time. This leads to a kinetic Monte Carlo algorithm and is suited for fast precipitation processes, only. Alternatively 2), Wallace and De Yoreo employed parallel replica simulations for an extensive sampling of configurations, thus mimicking infinite relaxation times.[21] Between these extremes, we suggest 3) a simulated-annealing-type procedure to allow aggregate relaxation to a degree that both energy profiles and aggregate structures evolve continuously as functions of nucleus size.[16]

Keywords: molecular simulation · nucleation · phase transitions · prenucleation clusters

[1] W. Ostwald, *Z. Phys. Chem.* **1897**, *22*, 289 – 330.
[2] N. Pienack, W. Bensch, *Angew. Chem. Int. Ed.* **2011**, *50*, 2014 – 2034; *Angew. Chem.* **2011**, *123*, 2062 – 2083.
[3] J. Anwar, D. Zahn, *Angew. Chem. Int. Ed.* **2011**, *50*, 1996 – 2014; *Angew. Chem.* **2011**, *123*, 2042 – 2061.
[4] P. Vekilov, *Nanoscale* **2010**, *2*, 2346 – 2357.
[5] D. Gebauer, H. Coelfen, *Nano Today* **2011**, *6*, 564 – 584.
[6] J. W. Gibbs, *Trans. Connect. Acad. Sci.* **1876**, *3*, 108 – 248.
[7] J. W. Gibbs, *Trans. Connect. Acad. Sci.* **1876**, *16*, 343 – 524.
[8] S. Auer, D. Frenkel, *Nature* **2001**, *413*, 711 – 713.
[9] I. N. Stranski, D. Totomanow, *Z. Phys. Chem.* **1933**, *163*, 399 – 408.
[10] P. E. Bonnett, K. J. Carpenter, S. Dawson, R. J. Davey, *Chem. Commun.* **2003**, 698 – 699.
[11] T. H. Zhang, X. Y. Liu, *Angew. Chem. Int. Ed.* **2009**, *48*, 1308 – 1312; *Angew. Chem.* **2009**, *121*, 1334 – 1338.
[12] P. G. Vekilov, *Cryst. Growth Des.* **2004**, *4*, 671 – 685.
[13] J. Anwar, P. K. Boateng, *J. Am. Chem. Soc.* **1998**, *120*, 9600 – 9604.
[14] P.Ectors, P.Duchstein, D.Zahn, *Cryst.Eng.Comm.* **2015**, DOI: 10.1039/C4CE02078B.
[15] J. A. Alonso, *Structure and Properties of Atomic Nanoclusters*, Imperial College Press, London, **2005**.
[16] T. Milek, P. Duchstein, G. Seifert, D. Zahn, *ChemPhysChem* **2010**, *11*, 847 – 852.
[17] L. Spanhel, *J. Sol-Gel Sci. Technol.* **2006**, *39*, 7 – 24.
[18] T. Schmidt, G. Müller, L. Spanhel, K. Kerkel, A. Forchel, *Chem. Mater.* **1998**, *10*, 65 – 71.
[19] D. Segets, A. Martin, J. Hartig, J. Gradl, W. Peukert, *Chem. Eng. Sci.* **2012**, *70*, 4 – 13.
[20] D. Gebauer, A. Völkel, H. Coelfen, *Science* **2008**, *322*, 1819 – 1822.
[21] A. F. Wallace, L. O. Hedges, A. Fernandez-Martinez, P. Raiteri, J. D. Gale, G. A. Waychunas, S. Whitelam, J. F. Banfield, J. J. De Yoreo, *Science* **2013**, *341*, 885 – 889.
[22] P. Raiteri, J. D. Gale, *J. Am. Chem. Soc.* **2010**, *132*, 17623 – 17634.
[23] R. Demichelis, P. Raiteri, J. D. Gale, D. Quigley, D. Gebauer, *Nat. Commun.* **2011**, *2*, 590.
[24] D. Gebauer, M. Kellermeier, J. D. Gale, L. Bergström, H. Coelfen, *Chem. Soc. Rev.* **2014**, *43*, 2348 – 2371.
[25] D. Erdemir, A. Y. Lee, A. S. Myerson, *Acc. Chem. Res.* **2009**, *42*, 621 – 629.
[26] J. Baumgartner, A. Drey, P. H. H. Bomans, C. Le Coadou, P. Fratzl, N. A. J. M. Sommerdijk, D. Faivre, *Nat. Mater.* **2013**, *12*, 310 – 314.
[27] W. Ostwald, *Z. Phys. Chem.* **1897**, *22*, 289 – 330.
[28] M. Mehring, *Coord. Chem. Rev.* **2007**, *251*, 974 – 1006.
[29] M. Walther, D. Zahn, *Eur. J. Inorg. Chem.* **2015**, 1178 – 1181.
[30] F. Bruneval, D. Donaldio, M. Parrinello, *J. Phys. Chem. B* **2007**, *111*, 12219.
[31] G. A. Tribello, C. Liew, M. Parrinello, *J. Phys. Chem. B* **2009**, *113*, 7081.
[32] H. Eyring, *Chem. Rev.* **1935**, *17*, 65 – 77.
[33] Q. Hu, M. H. Nielsen, C. L. Freeman, L. M. Hamm, J. Tao, J. R. I. Lee, T. Y. J. Han, U. Becker, J. H. Harding, P. M. Dove, J. J. De Yoreo, *Faraday Discuss.* **2012**, *129*, 164701.
[34] S. Auer, D. Frenkel, *J. Chem. Phys.* **2004**, *120*, 3015 – 3029.
[35] S. Auer, D. Frenkel, *Annu. Rev. Phys. Chem.* **2004**, *55*, 333 – 361.
[36] S. Auer, D. Frenkel, *Nature* **2001**, *409*, 1020 – 1023.
[37] F. Giberti, M. Salvalaglio, M. Parrinello, *IUCrJ* **2015**, *2*, 256 – 266.
[38] D. Moroni, P. R. ten Wolde, P. G. Bolhuis, *Phys. Rev. Lett.* **2005**, *94*, 235703.
[39] D. Zahn, *J. Phys. Chem. B* **2007**, *111*, 5249.
[40] D. Zahn, *J. Chem. Theory Comput.* **2006**, *2*, 107.
[41] D. Zahn, *Phys. Rev. Lett.* **2004**, *92*, 040801.
[42] A. Gavezzotti, G. Filippini, J. Kroon, B. P. van Eijck, P. Klewinghaus, *Chem. Eur. J.* **1997**, *3*, 893.
[43] A. Gavezzotti, *Chem. Eur. J.* **1999**, *5*, 567 – 576.
[44] A. Kawska, J. Brickmann, R. Kniep, O. Hochrein, D. Zahn, *J. Chem. Phys.* **2006**, *124*, 024513.

Received: March 17, 2015
Published online on April 27, 2015

